IET Optoelectronics

Research Article

IET Journals
The Institution of Engineering and Technology

Experimental demonstration of digital predistortion for orthogonal frequency-division multiplexing-radio over fibre links near laser resonance

ISSN 1751-8768
Received on 10th November 2014
Revised on 16th January 2015
Accepted on 21st February 2015
doi: 10.1049/iet-opt.2014.0160
www.ietdl.org

Luis Carlos Vieira[1,2] ✉, *Nathan Joseph Gomes*[1]

[1]*Broadband and Wireless Communications Group, University of Kent, Canterbury, Kent, CT2 7NT, UK*
[2]*Department of Electronics, Federal University of Technology – Paraná (UTFPR), Curitiba, 80230-901, Brazil*
✉ *E-mail: vieira@utfpr.edu.br*

Abstract: Radio over fibre (RoF), an enabling technology for distribution of wireless broadband service signals through analogue optical links, suffers from non-linear distortion. Digital predistortion has been demonstrated as an effective approach to overcome the RoF non-linearity. However, questions remain as to how the approach performs close to laser resonance, a region of significant dynamic non-linearity, and how resilient the approach is to changes in input signal and link operating conditions. In this work, the performance of a digital predistortion approach is studied for directly modulated orthogonal frequency-division multiplexing RoF links operating from 2.47 to 3.7 GHz. It extends previous works to higher frequencies, and to higher quadrature amplitude modulation (QAM) levels. In addition, the resilience of the predistortion approach to changes in modulation level of QAM schemes, and average power levels are investigated, and a novel predistortion training approach is proposed and demonstrated. Both memoryless and memory polynomial predistorter models, and a simple off-line least-squares-based identification method, are used, with excellent performance improvements demonstrated up to 3.0 GHz.

1 Introduction

Digital predistortion has been demonstrated as a compensation approach (at baseband) to overcome one of the most significant constraints of radio over fibre (RoF) technology as a transmission infrastructure option for wireless broadband access services – the RoF system non-linearity [1–7].

The analogue transmission in RoF systems enables simplification of remote antenna units (RAUs), with most of the signal processing performed at central base stations or central units (CUs) and at mobile terminals. Thus, small and lightweight RAUs can be used, which are less expensive than conventional base stations and can significantly reduce costs of site acquisition or leasing, and power consumption [8, 9]. In addition, the link transparency and the centralised processing also make network enhancements easier through only upgrading hardware/software at the central base stations [10].

The non-linearity of directly modulated RoF links comes mainly from the laser diode. Both third-order intermodulation distortion and relative intensity noise of lasers are frequency dependent, peaking at the relaxation frequency [11]. Orthogonal frequency-division multiplexing (OFDM) signals, commonly used in modern wireless systems, are particularly vulnerable to the link non-linearity, because of the high peak-to-average power ratio (PAPR) in their signal envelopes [12]. Thus, the RoF non-linearity may need to be compensated to achieve high dynamic range.

With digital predistortion, adaptive signal processing techniques are used to model, track and compensate the composite effects of the link non-linearity without the need for focusing on the characterisation of specific link components [1]. In seminal works, the performance of digital predistortion for directly modulated RoF links was evaluated by simulation using a non-linear RoF model [1, 3]. This model was extracted from measurements on a 1.8-GHz DFB RoF link of 2.2-km length and using a single-carrier quadrature phase shift keying input signal. The same model was used for the predistortion studies reported in [4].

The application of a memory-polynomial-based digital predistortion approach to directly modulated RoF links was introduced in [7], and experimentally demonstrated in [5, 6]. In [5], a preliminary result was reported, with mainly static RoF non-linearity reduced. Comparisons of adaptive algorithms and hardware implementation for the predistorter were considered in [6], with the RoF static non-linearity and the memory effects considerably reduced. In both [5, 6], however, the experiments were carried out only for a 6.25-MHz bandwidth OFDM signal, a quadrature amplitude modulation (QAM) level of 64, and at an intermediate frequency (IF) of 50 MHz. Moreover, the predistortion was tested for cases of only one [5] and two [6] average power levels. Error vector magnitude (EVM) results for the digital predistortion scheme applied to a 2.47-GHz OFDM-RoF link were recently reported [13]. However, those results were obtained from only one power level case and using only a QAM modulation level of 64. Thus, it is important to further demonstrate the predistortion performance for a wider range of experimental conditions and input signal parameters.

The work reported here represents a more complete demonstration of the memory polynomial predistortion approach to OFDM-RoF links compared with our previous works [5, 6, 13]. The novelty of the current work is summarised as follows: (1) the predistortion scheme is now tested significantly closer to (and around) the laser resonance frequency – it is well known that laser dynamic non-linearity peaks at resonance; (2) the first demonstration of the predistortion scheme for directly modulated RoF links using a 2048 IFFT size OFDM signal and 256 QAM modulation is achieved; (3) a high-power-level predistortion training approach is proposed and demonstrated; (4) the resilience of the predistortion approach to changes in modulation level of QAM schemes, and changes in average power levels are also studied. This resilience is important considering that, in such an off-line predistortion training scheme, the predistorter would not be trained continuously.

This paper is organised as follows. In Section 2, the performance metrics used in this work are defined. Then, the predistorter model

and identification method are discussed and the experimental setup presented in Section 3. In Section 4, the performance of OFDM-RoF links with digital predistortion are presented and discussed. Additional issues regarding linearisation of RoF systems are discussed in Section 5. Finally, the conclusions are presented in Section 6.

2 Performance metrics

To measure in-band signal performance in this work, we use the EVM – a metric commonly used in wireless communication standards [14, 15]. In this work, the EVM is calculated by

$$\mathrm{EVM}_{\mathrm{rms}} = \sqrt{\frac{(1/N)\sum_{k=1}^{N}(I_k - \overline{I}_k)^2 + (Q_k - \overline{Q}_k)^2}{(1/N)\sum_{k=1}^{N}(I_k^2 + Q_k^2)}} \quad (1)$$

where I_k is the in-phase ideal reference value of the kth symbol, Q_k is the quadrature ideal reference value of the kth symbol, $\overline{I}_k$ is the in-phase measured value of the kth symbol, $\overline{Q}_k$ is the quadrature measured value of the kth symbol and N is the length of the input vector. It should be noted that EVM can be calculated as either an equalised or unequalised value. In this work, as the focus is to observe the performance improvement in the RoF link because of the predistortion scheme only, no equalisation is applied to the output data sequence.

A widely used measure of spectral regrowth for communication systems is the adjacent channel power ratio (ACPR), a measurement of the effect of distortion components lying outside the signal bandwidth. The definition of ACPR depends on the system standard. Generally, it relates the ratio of the power in the adjacent channel (or out-of-band power) to the power in the channel under consideration (in-band power) [16]. The ACPR is given by

$$\mathrm{ACPR} = \frac{\int_{f_3}^{f_4} S_{xx}(f)\,\mathrm{d}f}{\int_{f_1}^{f_2} S_{xx}(f)\,\mathrm{d}f} \quad (2)$$

where f_1 and f_2 are the frequency limits of the channel under test, f_3 and f_4 are the frequency limits of the adjacent channel, and $S_{xx}(f)$ is the power spectral density (PSD) of the measured signal. In this work, the ACPR results are calculated by (2) with the channel under test and adjacent channels measured in a 18-MHz bandwidth and the lower and upper adjacent channels centred at −19 MHz and 19 MHz offset from the carrier frequency of the channel under test, respectively. All the EVM and ACPR results reported are averaged for 20 OFDM symbols.

3 Predistortion approach

In Fig. 1, a block diagram illustrating the digital predistortion scheme for RoF links is shown, considering the downlink direction. The digital predistorter, inserted before the RoF link (in baseband), is trained for executing the inverse function of the RoF link non-linearity so that the complete system is linearised. In the scheme of Fig. 1, the predistorter training block estimates the coefficients of the predistorter by comparing a feedback signal from the RAU with the original input signal. As a feedback connection, either a dedicated (linear) link or the RoF uplink can be used. If the latter option is chosen, there is no need to design/add any extra RoF link nor any related electronic converters at the central base station. However, the non-linearities that stem from the RoF uplink itself may need to be compensated [7].

The indirect learning architecture [17] is commonly used for predistortion identification (training) schemes [2, 6, 18]. With this architecture, and assuming that the system non-linearity does not change rapidly with time, it is possible to implement the predistortion training off-line. It is important to consider field implementation of the predistorter: the complexity and cost of the compensation scheme can be reduced if the predistorter is trained in such an off-line manner as it eliminates the need for implementing parameter-estimation algorithms in hardware [19]. This refers only to the implementation of the predistorter training block in Fig. 1. In the diagram of Fig. 1, when the error $e(n)$ between the predistorter output $z(n)$ and the predistorter training block output $\hat{z}(n)$ is minimised, the predistorter coefficients are estimated by the training block, and are then used for updating the predistorter. For demonstration purposes the digital predistorter block might process the input data in software (off-line). In a real system, however, it would be done through a real-time hardware implementation.

In this work, the predistortion identification scheme is based on the indirect learning architecture, with a specific in-house time alignment algorithm (see Section 3.2) in conjunction with the off-line least squares (LS) method (see Section 3.1) used. The methodology used for 'training' the predistorter is similar to that used for 'modelling' of RoF link distortion in [20]. However, no predistortion scheme was tested in [20].

3.1 Predistorter model and its identification

In this work, a memory polynomial structure has been chosen as the predistorter model. The memory polynomial is considered to be one of the most powerful and robust models for both direct and inverse modelling of power amplifier non-linearity [21]. This model captures memory effects with lower number of coefficients compared with the more general Volterra model and can be estimated using a simple, least-squares method [18]. It should be noted that, for RoF links, a memoryless model may not be able to describe the electro-optical conversion process properly [22]. An additional advantage, considering the realisation of the off-line

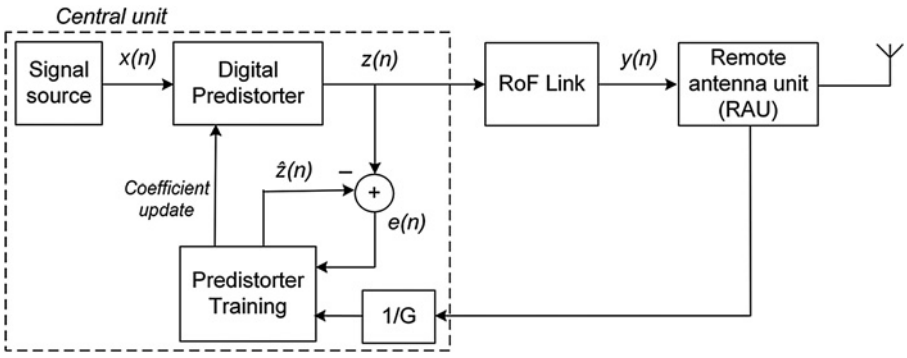

Fig. 1 *Block diagram of digital predistortion approach*
G = RoF link gain

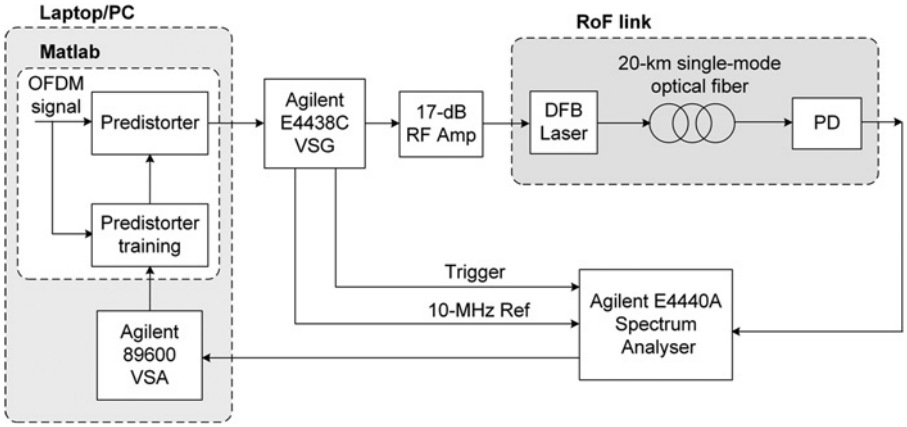

Fig. 2 *Experimental setup for digital predistortion of OFDM RoF links*
PD = Photodiode

predistortion experiments, is the fact that the memory polynomial model can be easily converted to a memoryless polynomial one, allowing the same algorithm to be used for comparative experiments between the memory and memoryless predistortion approaches. In the diagram shown in Fig. 1, the predistorter output $z(n)$ is given by [18]

$$z(n) = \sum_{k=1}^{K} \sum_{q=0}^{Q} c_{kq} x(n-q) \left| x(n-q) \right|^{k-1} \tag{3}$$

where $x(n-q)$ is the input signal delayed by q sample periods, K is the nonlinearity order, Q is the memory length and c_{kq} are the predistorter coefficients. The predistorter identification procedure is based on the LS method and is described below, following the explanation in [18].

At first, let us collect the coefficients c_{kq} into a vector $\boldsymbol{c}$ as in

$$\boldsymbol{c} = \left[c_{10}, \ \ldots, c_{K0}, \ \ldots, c_{1Q}, \ \ldots, c_{KQ} \right]^{\mathrm{T}} \tag{4}$$

Each component of the coefficient vector $\boldsymbol{c}$ is associated with a signal whose time samples over the period N are collected into the vector

$$\boldsymbol{U}_{kq} = \left[u_{kq}(n), u_{kq}(n+1), ..., u_{kq}(n+N-1) \right]^{\mathrm{T}} \tag{5}$$

in which

$$u_{kq}(n) = \frac{y(n-q)}{G} \left| \frac{y(n-q)}{G} \right|^{k-1} \tag{6}$$

where $y(n-q)$ is the RoF output signal delayed by q sample periods and G is the RoF link gain (see Fig. 1).

Assembling all vectors $\boldsymbol{U}_{kq}$ into a matrix $\boldsymbol{U}$ such that the model can be compactly expressed as

$$\hat{\boldsymbol{z}} = \boldsymbol{U}\boldsymbol{c} \tag{8}$$

where $\hat{\boldsymbol{z}}$ is an $N \times 1$ vector that represents an estimate of the actual vector $\boldsymbol{z}$. The estimation vector error for a block of N samples is

$$\boldsymbol{e} = \boldsymbol{z} - \hat{\boldsymbol{z}} \tag{9}$$

Finally, the least-squares solution that minimises the error is given by

$$\boldsymbol{c} = \left(\boldsymbol{U}^{\mathrm{H}} \boldsymbol{U} \right)^{-1} \boldsymbol{U}^{\mathrm{H}} \boldsymbol{z} \tag{10}$$

where $[\cdot]^{\mathrm{H}}$ denotes complex conjugate transpose.

3.2 Experimental setup

The setup used for the predistortion performance experiments is depicted in Fig. 2. The OFDM signal is set either with 256- or 2048-point IFFT size, 18-MHz bandwidth (total). Four times oversampling is employed. Modulation levels of 16, 64 or 256 QAM are used. The OFDM signal is modulated onto RF carrier frequencies of 2.47, 2.6, 2.8, 3.0 or 3.7 GHz by an Agilent E4438C VSG and transmitted through the RoF link. Even the lowest-used RF carrier frequency is higher than that used in [1, 3, 4] and significantly higher than the IF carrier frequency employed in [5, 6]. At the link output, an Agilent E4440A spectrum analyser and Agilent 89600 VSA software are used to measure the output signal. The RoF link consists of a directly modulated 1311-nm DFB laser, model EmCore 1935F, a 20-km length single-mode optical fibre and an Appointech InGaAs PIN photodiode with (3-dB RF) bandwidth of 4.3 GHz and responsivity around 1 A/W. The laser, which has a threshold current of 8 mA and slope efficiency of 0.18 W/A, is set at a bias current of 30 mA where its output power is around 4 mW and its relaxation resonance is around 3.8 GHz. A 17-dB amplifier, model SHF Communication Technologies SHF 824, with frequency range from 30 kHz to 30 GHz and 1-dB compression point of 26 dBm (output) is used to drive the laser into its nonlinear region. In [7], we studied adaptive predistortion schemes for the joint compensation of RoF and power amplifier non-linearities. In the current work, the impact of the amplifier on the overall link performance is neglected since the amplifier operates within its linear region for the signal PAPRs and average power levels used.

The predistortion experiments were carried out in two steps: a training phase, for predistorter parameter identification; and a testing phase, for comparison of the non-predistorted against the

$$\boldsymbol{U} = \begin{bmatrix} u_{10}(n) & \cdots & u_{K0}(n) & \cdots & u_{1Q}(n) & \cdots & u_{KQ}(n) \\ u_{10}(n+1) & \cdots & u_{K0}(n+1) & \cdots & u_{1Q}(n+1) & \cdots & u_{KQ}(n+1) \\ \vdots & & \vdots & & \vdots & & \vdots \\ u_{10}(n+N-1) & \cdots & u_{K0}(n+N-1) & \cdots & u_{1Q}(n+N-1) & \cdots & u_{KQ}(n+N-1) \end{bmatrix} \tag{7}$$

predistorted link performances. It should be noted that two different pseudo-random data sequences for the OFDM signals were used for each phase.

The time delay between the input and output baseband signals needs to be accurately estimated and compensated before predistorter identification [23]. In the current work, the time-domain input-output OFDM signals are time-aligned using an in-house alignment algorithm in Matlab. This algorithm is based on the cross-correlation between the input-output signals for time-delay estimation and includes interpolation for a better accuracy. The interpolation was applied to the four times oversampled signals, increasing their sampling rate for the identification by 10. This is a low-pass interpolation technique performed by inserting zeros between the original data values and then applying a low-pass finite impulse response filter [24]. A fine alignment between the input-output signals is achieved by estimating the delay between the input-output interpolated data via cross-correlation and then time shifting one of the data sequences. Then, the sampling rate of the time-aligned signals is returned to the original value by using a decimation technique by which the data sequences are low-pass filtered and then down-sampled. After the alignment procedure, the predistorter coefficients of (3) are estimated in the predistorter training block (Fig. 2) using the LS-based identification algorithm described in Section 3.1.

For the testing phase, the predistorter coefficients obtained in the training phase are used in the predistorter block for generating the predistorted OFDM signal (in Matlab). This signal is then downloaded to the VSG and transmitted through the RoF link, with the performance of the predistorted link compared against that of the non-predistorted link.

4 Digital predistortion results

4.1 Predistortion performance and RF input power

In this section, experimental and simulation studies considering the effects of the average RF power level on the digital predistortion performance for directly modulated RoF links are reported. Two sets of experiments are reported each using a different predistortion training scheme. The OFDM signal is set with 256-point IFFT size and has a baseband PAPR of around 9.5 dB. The data modulation level is 64 QAM. The experiments were carried out at the RF frequency of 2.47 GHz and the average power range (at the laser input) from –2 to 3 dBm. This range is chosen (and is specific to this laser/link) because the non-linearity has insignificant effect on EVM below –2 dBm, while above 3 dBm we know that the non-linearity is so significant that it would require very complex and cumbersome predistortion, if it is possible at all. Nevertheless, the possibility of extending the operational range by a few dB can have significant benefits on the overall system design and performance. We note that the average power range used in this work is 2 dB wider than that used in our previous work [6]. The frequency of 2.47 GHz is used to demonstrate the predistortion approach within the band of WiFi and WiMAX networks. The performance results are for the predistorter model of (3) with Q set to either 0 or 2 and K set to 7.

The measured EVM results are shown in Fig. 3, including the predistorted EVMs for a conventional training approach and for a novel, high-power-level predistortion training approach. The non-predistorted EVM increases from 3.3 to 10.6% with increase in the average RF input power. For each training approach, the memory polynomial predistorter ($Q = 2$) performs better than the memoryless one ($Q = 0$), although the differences are not very significant.

Let us consider, at first, the conventional training approach (labelled as 'Training A' in Fig. 3). Here, the predistorter is trained from the measurements at each average RF power level, that is, the predistorter coefficients are updated for each input power case. With this training approach and up to the power level of 1 dBm, the predistorted EVM is more than halved. Thus, the EVM results in Fig. 3 show that the conventional predistortion training

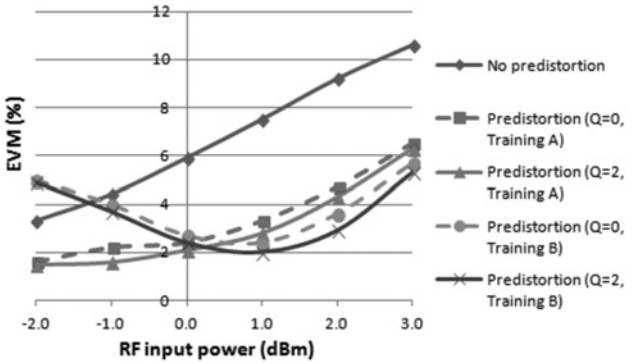

Fig. 3 *Measured EVM results due to RF input power for the RoF output without predistortion, with memoryless ($Q = 0$) and memory ($Q = 2$) predistortion*

Conventional (Training A) against high-power-level (Training B) predistortion training approaches
RF carrier = 2.47 GHz, PAPR (input signal) = 9.5 dB, $K = 7$

technique can improve the RoF link performance very well up to some degree of link distortion. Additional predistortion tests were carried out using $Q = 2$ and $K = 11$ and with $Q = 16$ and $K = 11$, with the same EVM results obtained as for $Q = 2$ and $K = 7$ (within 0.1% of accuracy). The performance improvement becomes less significant for very highly distorted links, this is because of the limitations of: (1) the power-series based models in representing highly distorted systems (e.g. a hard-clipped system); (2) the off-line predistortion training approach in dealing with fast changes in link non-linearity, for example because of laser gain drift; (3) the measurement system in accurately characterising the system non-linearity. This accuracy is limited by the linearity and bandwidth of the measurement system [23].

Some simulation results are reported in Fig. 4, for a comparison with the measured results. To obtain the simulated EVMs, a memory polynomial model (with $Q = 2$ and $K = 7$) was extracted from the measured data at 3-dBm power level, using the behavioral modelling approach [12, 20]. This model was then used to simulate the RoF link non-linearity at the six power level cases by scaling the input signal accordingly. Finally, the predistorted RoF link was simulated by inserting the predistorter model of (3) before the RoF model. The predistorter model was trained for each power level case, with $Q = 2$ and $K = 7$, using the identification method described in Section 3. As shown in Fig. 4, there is an excellent match between simulated and measured EVMs.

In a real system, the signal levels may fluctuate leading to variations in the degree of the distortion experienced through the RoF link. Thus, it is unclear how well the predistortion scheme will work (at least until re-trained) when this occurs. To

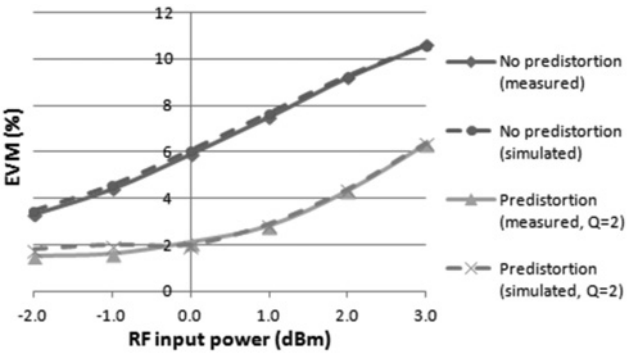

Fig. 4 *Measured against simulated EVM results due to RF input power for the RoF output without predistortion and with memory predistortion ($Q = 2$)*

Predistorter trained for each power level case (conventional training)
RF carrier = 2.47 GHz, PAPR (input signal) = 9.5 dB, $K = 7$

investigate this issue and in an attempt to further improve the digital predistortion performance, the high-power-level predistortion training approach is proposed and demonstrated. With this approach, the predistorter is trained for a single, high average RF power level at the laser input, and the coefficients obtained are applied to compensate a RoF link operating at lower power levels. To the best of the authors' knowledge, this is the first demonstration of such a predistortion training approach to RoF systems.

Considering the EVM results for the high-power-level predistortion training approach in Fig. 3 (labelled as 'Training B'), the predistorter coefficients are obtained with the RF average power set to 4 dBm at the laser input. This training approach allows for better predistortion performance when the link distortions are high, such as for the 1-, 2- and 3-dBm power level cases. However, the predistortion performance degrades for the lower power level cases. We analysed the input-output characteristics of the predistorted link and observed that the predistorter actually overcompensates the RoF link for the power level cases of −2, −1 and 0 dBm. The EVM results for the high-power-level training also show that the off-line predistortion training approach can cope with some range of RF drive level variation at the laser input, as long as the requirement is to meet a particular level of EVM rather than its absolute minimisation.

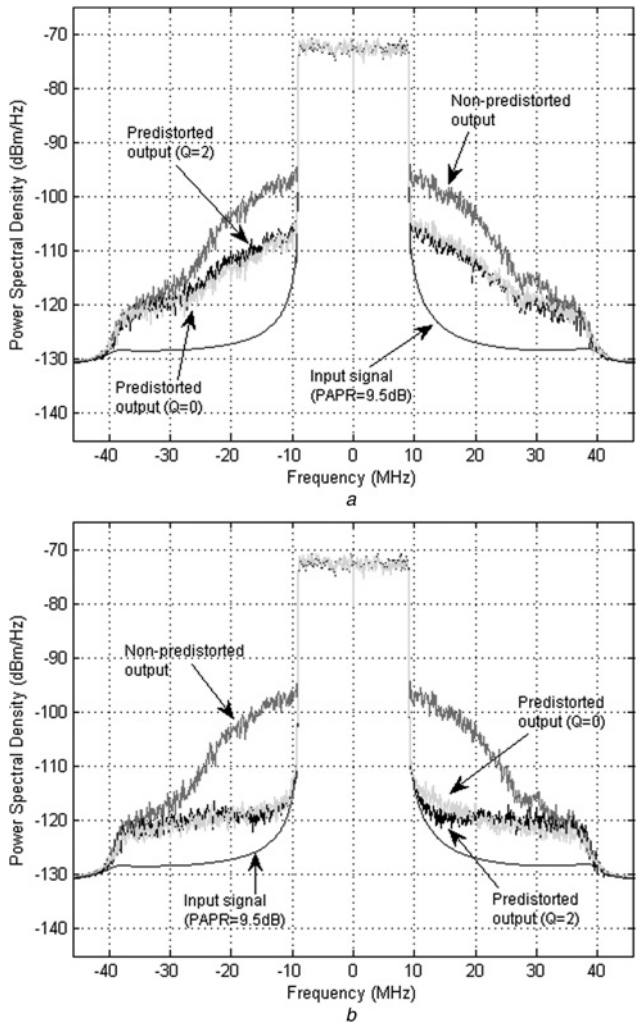

Fig. 5 *Measured PSD plots of the RoF link output without predistortion, with memoryless (Q = 0) and memory (Q = 2) predistortion*

RF carrier = 2.47 GHz, RF input power = 1 dBm. Predistorter trained at
a 1 dBm
b 4 dBm

Table 1 EVM and ACPR results at higher RF carrier frequencies

RF carrier, GHz	2.6	2.8	3.0	3.7
non-predistorted EVM, %	4.4	4.1	5.9	13.2
predistorted EVM, %, $Q = 0$	3.1	2.8	1.9	11.0
predistorted EVM, %, $Q = 2$	1.6	1.6	1.7	10.8
non-predistorted lower/	−35.5/	−35.4/	−31.0/	−21.7/
upper ACPR, dBc	−35.9	−35.0	−31.0	−20.9
predistorted lower/upper	−47.5/	−46.0/	−45.5/	−23.9/
ACPR, dBc, $Q = 0$	−47.5	−46.4	−43.7	−23.2
predistorted lower/upper	−47.2/	−46.7/	−45.0/	−23.9/
ACPR, dBc, $Q = 2$	−47.3	−46.8	−44.7	−23.1

Predistorter trained for each frequency case. PAPR (input signal) = 9.5 dB.

Significant reductions in the level of spectral regrowth because of digital predistortion can be seen in the PSD plots of Fig. 5. These spectra are for the 1-dBm power level case, with the predistorter trained for a drive level of either 1 or 4 dBm at the laser input, shown in Figs. 5*a* and *b*, respectively. It should be noted that similar spectral performance is achieved by both the memoryless ($Q = 0$) and memory ($Q = 2$) predistorter models. For the experimental case of Fig. 5, the high-power-level predistortion training (Fig. 5*b*) gives better results compared with the conventional training approach (Fig. 5*a*). For example, the upper ACPR (integrated from 10 to 28 MHz) is reduced by 9.3 dB because of memory predistortion using the conventional training method while it is reduced by 17.2 dB using the high-power-level training approach.

A solution to improve the performance of the high-power-level predistortion training approach for OFDM-RoF links operating well below the predistortion training power level, that is, weakly distorted links, is now presented. In this proposal, the input signal is scaled down prior to the signal being processed by the predistorter so that the average power is backed off from the nonlinear region of the predistorter characteristics. In this way, the predistortion effect on the input signal can be reduced, thus decreasing the overcompensation effect on the RoF link and improving the predistortion performance. We note that the baseband signal is scaled up after the predistorter.

By using the simulation scheme previously described, we tested the scaled-down version of the high-power-level predistortion training approach for the power level cases of −1 and −2 dBm. The predistorter model was extracted from the measured data at 4-dBm power level, with $Q = 2$ and $K = 7$. The signal power was reduced (just for passing through the predistorter) by 1 and 1.8 dB for the −1- and −2-dBm power level cases, respectively, with the corresponding predistorted EVMs of 1.6 and 1.9% obtained. The dynamic range was not reduced using this approach as the (baseband) signal power was increased by the respective 1 and 1.8 dB after the predistorter. These EVM results are significantly better than the measured EVMs shown in Fig. 3 for the power level cases considered, indicating that the high-power-level predistortion training technique can be applied for a wide range of input powers by properly scaling the input signal.

4.2 Performance at higher RF carrier frequencies

Experimental results at the frequencies of 2.6, 2.8 and 3.0 GHz are reported to demonstrate the digital predistortion scheme for the RoF link operating in a region of the laser response below (but not so far from) the laser resonance region. The measured frequency response of the 20-km length RoF link for the bias current of 30 mA is shown in Fig. 6, where it can be seen that the laser resonance is around 3.8 GHz. The predistortion approach was also tested within the laser resonance region at 3.7 GHz, as a special case. Considering that low-cost semi-conductor lasers are readily available with an upper modulation frequency limit of around 3 GHz [25] and that directly modulated RoF links are generally set up well below the laser resonance, the linearisation technique could make it possible to extend the maximum operating frequency of these low-cost RoF links. The OFDM signal, set with

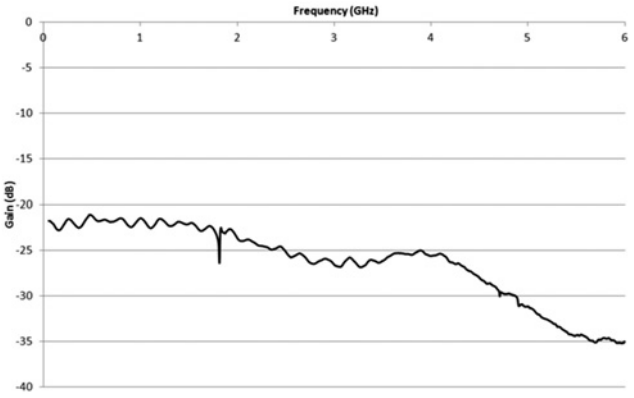

Fig. 6 *Measured frequency response of the 20-km length RoF link*
Bias current = 30 mA

256-point IFFT size, has a baseband PAPR of around 9.5 dB. The modulation level of 64 QAM is used. The predistorter model of (3) is set either with $Q = 0$ or $Q = 2$ and with $K = 7$.

In Table 1, the EVM and ACPR results for the higher frequency cases and for the average power level of 0 dBm at the laser input are listed. These results show that significant performance improvement can be achieved using the digital predistortion technique up to 3.0 GHz. At this frequency, for example, the EVM is reduced to less than a third because of the predistortion approach. In terms of EVM, better performance is achieved using the memory polynomial model as predistorter, especially for the 2.6- and 2.8-GHz cases for which the EVM results are almost halved in comparison with the results using the memoryless polynomial model. In terms of ACPR metric, the digital predistorter performs quite similarly using either memory or memoryless polynomial models. This indicates that the memory polynomial predistorter is more effective in reducing in-band than out-of-band distortion. The excellent reduction in the RoF link spectral regrowth because of the digital predistortion approach can be seen in Fig. 7, for the 3.0-GHz frequency case, as an illustrative example.

As shown in Table 1, only slight EVM and ACPR reduction is achieved at the frequency of 3.7 GHz. This can be explained by the fact that the polynomial model does not cope very well with the high level of link distortion around the laser resonance. We observed the link distortion by measuring the input-output characteristics of the RoF link at 3.7 GHz. Another predistortion

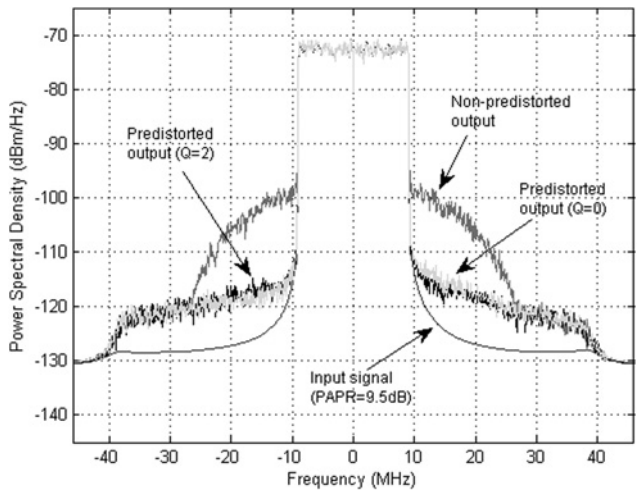

Fig. 7 *PSD plots of the 64-QAM/256-OFDM RoF link without predistortion, with memoryless (Q = 0) and memory (Q = 2) predistortion*
RF carrier = 3.0 GHz, RF input power = 0 dBm

Table 2 EVM results for the 256-QAM/2048-OFDM RoF link

RF input power, dBm	0.0	1.0
non-predistorted EVM, %	5.1	6.0
(a) Predistorted EVM, %	2.2	3.4
(b) Predistorted EVM, %	2.5	3.6

(a) Predistorter trained for a 256-QAM/2048-OFDM signal.
(b) Predistorter trained for a 16-QAM/2048-OFDM signal.
PAPR (input test signal) = 10.7 dB.

experiment was also carried out at 3.7 GHz with the average input power reduced by 1 dB. For this case, the non-predistorted EVM of 10.3% was significantly reduced to 4.4% using the memory-polynomial-based predistorter. Thus, these results indicate that the digital predistortion scheme can improve the link performance even at the laser resonance frequency, but performance is very dependent on the average RF input power. While this dependence also occurs for frequencies below the laser resonance, see for example the EVM results for 2.47 GHz in Fig. 3, it is clear that the performance changes more dramatically at resonance.

4.3 Predistortion experiments for 256-QAM/2048-OFDM RoF links

In modern wireless communications systems the QAM modulation scheme may be varied. For example, control/protocol overheads may be sent with lower QAM than user data, even for users with good wireless channel conditions. Thus, it is important to observe the performance of the digital predistortion technique for RoF links with the predistorter trained for a different QAM level than that of the signal to be predistorted. In this section, the performance of the digital predistortion approach applied to a 256-QAM/2048-OFDM RoF link using either 16-QAM or 256-QAM modulation level in the OFDM training signal are compared. The results also demonstrate the use of the digital predistortion scheme for RoF links transmitting with such high QAM level and large FFT size OFDM signals.

The experiments were carried out at the RF frequency of 2.47 GHz and average power levels of either 0 or 1 dBm at the laser input. The 256-QAM/2048-OFDM test signal has a baseband PAPR of around 10.7 dB. The EVM results are shown in Table 2, with the predistorted EVMs for the 256-QAM/2048-OFDM training signal listed in the third row and for the 16-QAM/2048-OFDM training signal listed in the fourth row. These results are for a memory-polynomial-based predistorter trained for each average power level, with Q set to 2 and K set to 7. From Table 2, it can be seen that similar EVM results are obtained using either the 16-QAM/2048-OFDM or the 256-QAM/2048-OFDM training signal, indicating that the digital predistortion approach is resilient to changes in the QAM modulation level.

5 Further discussion

Considering the distortion compensation of bidirectional RoF links, asymmetric schemes using digital predistortion for the downlink direction and postdistortion for the uplink direction have been proposed [1, 7]. With this asymmetric approach, the compensation of the RoF up/downlink non-linearities is concentrated at the central base stations (in baseband) so that the increase in the complexity/cost of the RAUs is minimised. Another advantage of implementing the pre/postdistortion scheme is that a postdistorted uplink can be used as a linear feedback connection for training the predistorter [1].

It is worth noting that the impact of latency introduced by the predistorter on OFDM-RoF systems can be made insignificant. Latency depends on the number of predistorter coefficients and the hardware implementation. In the current work, the digital predistorter pre-processes the input signal in software (off-line). In [6], however, a fifth order predistorter was implemented in FPGA

hardware with a latency of 62.5 ns (five clock cycles), showing that the latencies induced are more than an order of magnitude (perhaps two orders of magnitude) less than the OFDM symbol duration.

Multi service systems, with different signal PAPRs involved, have not been considered in this work. However, as future work, we can combine the digital predistortion approach with some PAPR reduction technique in a multi service system to maintain the PAPR value of each input signal below a certain level and obtain good predistortion performance. For this type of system, however, the digital predistorter would need to be performed on the baseband signal of each RF sub-band, which would make the training of each sub-band predistorter more challenging compared with the predistortion training for a single band OFDM-RoF system. This is mainly because the intermodulation distortion on a specific sub-band coming from other RF sub-bands needs to be considered when the predistorter coefficients for that specific sub-band are obtained.

6 Conclusion

To the best of the authors' knowledge, this work reports the first experimental demonstration of the digital predistortion technique for directly modulated OFDM-RoF links operating near laser relaxation resonance. Excellent performance improvements have been shown up to 3.0 GHz, which corresponds to around 4/5 of the laser resonance (3.8 GHz). Although some of the results suggest that the digital predistortion approach might be applied even for RoF links operating at the laser resonance, further studies in this frequency region are still necessary.

Both memoryless and memory polynomial predistorter models and a simple off-line LS-based identification algorithm have been used. For most of the experimental cases, the memory polynomial predistorter performed better than the memoryless one in terms of EVM, while the two predistorter models showed similar results for the reduction in spectral regrowth.

The performance of the digital predistortion approach to 64QAM/OFDM RoF links has been evaluated considering the (average) RF power level, with a (novel) high-power-level predistortion training method proposed and demonstrated. Compared with a conventional training method, better EVM and spectral power leakage results were achieved using the novel predistortion training for strongly distorted link operation. Importantly, the results reported also show that the off-line predistortion training method can cope with a range of average RF power variation of a few dB at the laser input. In addition, a solution to improve the performance of the novel predistortion approach for weakly distorted links has been proposed.

The first demonstration of the digital predistortion approach to directly modulated RoF links using a 2048 IFFT size OFDM test signal and 256-QAM modulation level has been achieved. The promising performance improvements found indicate that the digital predistortion technique can be applied to RoF systems in an environment of high-data-rate, wideband communication systems. In addition, the resilience of the predistortion approach to changes in the QAM modulation level has been demonstrated.

7 Acknowledgments

The authors would like to thank Anthony Nkansah for developing the Simulink model used for generating the user-defined OFDM signals. This work was partially supported within the framework of the European Union Integrated Project FUTON (FP7 ICT-2007-215533). The work of Luis C. Vieira was supported by the Brazilian Government through CNPq and UTFPR.

8 References

1 Fernando, X.N., Sesay, A.B.: 'Adaptive asymmetric linearization of radio over fiber links for wireless access', *IEEE Trans. Veh. Technol.*, 2002, **51**, (6), pp. 1576–1586
2 Hekkala, A., Lasanen, M.: 'Performance of adaptive algorithms for compensation of radio over fiber links'. Proc. IEEE Wireless Telecommunication Symp., Prague, Czech Republic, April 2009, pp. 1–5
3 Fernando, X.N., Sesay, A.B.: 'Higher order adaptive filter based predistortion for nonlinear distortion compensation of radio over fiber links'. Proc. IEEE Int. Conf. on Communications, ICC 2000, New Orleans, LA, June 2000, pp. 367–371
4 Moon, H., Sedaghat, R.: 'FPGA-Based adaptive digital predistortion for radio-over-fiber links', *Microprocess. Microsyst.*, 2006, **30**, (3), pp. 145–154
5 Vieira, L.C., Gomes, N.J., Nkansah, A.: 'An experimental study on digital predistortion for radio-over-fiber links'. Proc. SPIE 7988, Optical Transmission Systems, Switching, and Subsystems VIII, February 2011, p. 798828, doi: 10.1117/12.888602
6 Hekkala, A., Hiivala, M., Lasanen, M., *et al.*: 'Predistortion of radio over fiber links: algorithms, implementation, and measurements', *IEEE Trans. Circuits Syst. I: Regul. Pap.*, 2012, **59**, (3), pp. 664–672
7 Hekkala, A., Lasanen, M., Vieira, L.C., Gomes, N.J., Nkansah, A.: 'Architectures for joint compensation of RoF and PA with nonideal feedback'. Proc. 2010 IEEE 71st Vehicular Technology Conf., VTC-Spring 2010, Taipei, Taiwan, May 2010, pp. 1–5
8 Kim, H., Cho, J.H., Kim, S., *et al.*: 'Radio-over-fiber system for TDD-based OFDMA wireless communication systems', *J. Lightwave Technol.*, 2007, **25**, (11), pp. 3419–3427
9 Liu, C., Zhang, L., Zhu, M., Wang, J., Cheng, L., Chang, G.-K.: 'A novel multi-service small-cell cloud radio access network for mobile backhaul and computing based on radio-over-fiber technologies', *J. Lightwave Technol.*, 2013, **31**, (17), pp. 2869–2875
10 Wake, D.: 'Trends and prospects for radio over fibre picocells'. Proc. Int. Topical Mtg. on Microwave Photonics, Awaji, Japan, November 2002, pp. 21–24
11 CoxIIIC.H.: 'Analog optical links: Theory and practice' (Cambridge University Press, 2004)
12 Vieira, L.C., Gomes, N.J., Nkansah, A., van Dijk, F.: 'Behavioral modeling of radio-over-fiber links using memory polynomials'. Proc. IEEE Int. Topical Meeting on Microwave Photonics, MWP 2010, Montreal, Canada, October 2010, pp. 85–88
13 Gomes, N.J., Assimakopoulos, P., Vieira, L.C., Sklikas, P.: 'Fiber link design considerations for cloud-radio access networks (Invited Paper)'. Proc. IEEE Int. Conf. on Communications, ICC 2014, Sydney, Australia, June 2014, pp. 382–387
14 3GPP TS 36.104: 'Evolved universal terrestrial radio access (E-UTRA); Base station (BS) radio transmission and reception', version 8.12.0 Release 8, 2011
15 IEEE Std 802.16™-2009: 'IEEE standard for local and metropolitan area networks; Part 16: Air interface for broadband wireless access systems', 2009
16 Song, J.B., Islam, A.H.M.R.: 'Distortion of OFDM signals on radio-over-fiber links integrated with an RF amplifier and active/passive electroabsorption modulators', *J. Lightwave Technol.*, 2008, **26**, (5), pp. 467–477
17 Eun, C., Powers, E.J.: 'A new Volterra predistorter based on the indirect learning architecture', *IEEE Trans. Signal Process.*, 1997, **45**, (1), pp. 223–227
18 Ding, L., Zhou, G.T., Morgan, D.R., *et al.*: 'A robust digital baseband predistorter constructed using memory polynomials', *IEEE Trans. Commun.*, 2004, **52**, (1), pp. 159–165
19 Zhu, A., Draxler, P.J., Yan, J.J., Brazil, T.J., Kimball, D.F., Asbeck, P.M.: 'Open-loop digital predistorter for RF power amplifiers using dynamic deviation reduction-based Volterra series', *IEEE Trans. Microw. Theory Tech.*, 2008, **56**, (7), pp. 1524–1534
20 Vieira, L.C., Gomes, N.J.: 'Baseband behavioral modeling of OFDM-radio over fiber link distortion'. Proc. IEEE Int. Topical Meeting on Microwave Photonics, MWP 2012, Noordwijk, The Netherlands, September 2012, pp. 188–191
21 Hammi, O., Ghannouchi, F.M., Vassilakis, B.: 'A compact envelope-memory polynomial for RF transmitters modeling with application to baseband and RF-digital predistortion', *IEEE Microw. Wirel. Compon. Lett.*, 2008, **18**, (5), pp. 359–361
22 Shah, A.R., Jalali, B.: 'Adaptive equalisation for broadband predistortion linearisation of optical transmitters', *IEE Proc. Optoelectron.*, 2005, **152**, (1), pp. 16–32
23 Ghannouchi, F.M., Hammi, O.: 'Behavioral modeling and predistortion', *IEEE Microw. Mag.*, 2009, **10**, (7), pp. 52–64
24 Coleri, S., Ergen, M., Puri, A., Bahai, A.: 'Channel estimation techniques based on pilot arrangement in OFDM systems', *IEEE Trans. Broadcast*, 2002, **48**, (3), pp. 223–229
25 Wake, D., Nkansah, A., Gomes, N.J.: 'Radio over fiber link design for next generation wireless systems', *J. Lightwave Technol.*, 2010, **28**, (16), pp. 2456–2464